8.8

NUMERICAL INVESTIGATION OF COUPLED BOUNDARY LAYERS AIR-SEA TRANSFER (CBLAST) AT SMALL SCALES

Song Liu[1], Kelli Hendrickson[1], Xiaoxia Dong[1], Lian Shen[2] and Dick K.P. Yue[1]

[1]Department of Ocean Engineering, Massachusetts Institute of Technology, Cambridge, MA

[2]Department of Civil Engineering, the Johns Hopkins University, Baltimore, MD

1. INTRODUCTION

The understanding and prediction of the coupled dynamics of atmosphere-ocean-wave interactions are of vital importance to environmental applications such as global warming and pollutant transport as well as Navy operations. Due to the complex nature of the air-water interactions, our current understanding of the mechanisms for the transport of mass, momentum and heat within the atmosphere-ocean wave boundary layer (WBL) is quite limited. There is a critical need for a detailed investigation of the small-scale physics, which is essential for the understanding of the air-sea coupling dynamics and is the foundation for the development of parameterization tools.

In this study, we investigate the dynamics of atmosphere-ocean-wave interactions by performing direct numerical simulation (DNS) and large-eddy simulation (LES) for both the air and ocean turbulent flows with coupled free-surface boundary conditions. We focus on small spatial scales on the order of a surface wave length, and low to moderate wind speeds (O(2~5)m/s) corresponding to Reynolds numbers $Re \sim O(10^{5\sim6})$. The transport of passive scalars by the air and water is also simulated. Through high-resolution DNS and LES, we obtain a complete physical description of the turbulent air-sea flow field, which establishes a basis for the identification of key transport processes within the WBL and for the parameterization. Based on the extensive simulation results obtained, we further develop formulation for the Reynolds-averaged Navier-Stokes (RANS) simulation of the air-water mixed flow and physics-based RANS modeling.

2. SIMULATION APPROACHES

We employ a systematic approach for the simulation of coupled air-water turbulent flows. At low Reynolds numbers, DNS, which does not require any turbulence closure, is performed to obtain the "true" physical mechanisms and structures as well as statistical description of the flow field. At moderate Reynolds numbers, we perform LES, of which only the large-scale motions are simulated directly while the effects of small sub-grid scale (SGS) are modeled. As shown by Shen & Yue (2001), physics-based SGS modeling is the key to the success of LES of air-water free-surface flows. Based on the physical insights obtained from DNS and LES, we further develop RANS modeling for the parameterization of the air-sea coupled flows at high Reynolds numbers corresponding to large spatial scales.

To simulate the air-water coupled viscous flows with a free interface, we develop a suite of novel numerical capabilities. At low Froude numbers where the free-surface deformation is small, we employ a boundary interface tracking method (BITM) which utilizes coupled free-surface boundary conditions to capture the interactions between the air and water motions. The primitive-variable form of the Navier-Stokes equations is solved for the air and water motions respectively. At the free surface, we employ a kinematic boundary condition requiring that the interface remains a material surface, and dynamic boundary conditions requiring a stress balance across the interface. The governing equations are discretized using a pseudo-spectral method in the horizontal directions and a finite-difference scheme in the vertical direction. A second-order fractional-step scheme is used for the time integration of the flow field.

For moderate to large Froude numbers where the surface waves steepen and break, we develop an Eulerian interface capturing method (EICM) based on a level set approach. In EICM, the air and water together are treated as a system with varying density and viscosity. A continuous scalar, the level set function representing the signed distance from the interface, is used to identify each fluid. The fluid motions are governed by the Navier-Stokes equations while the scalar is advected with the flow governed by a Lagrangian-

invariant transport equation. The governing equations are discretized on an Eulerian grid using a finite-difference scheme.

3. RESULTS

As two canonical problems, coupled air-water turbulent Couette flows and unsteady spilling breaking waves are simulated in this study. By investigating these two cases, we are able to separate and identify the effects of air-water viscous coupling and the effects of wave-turbulence interactions, which are essential for the development of physics-based turbulence modeling.

3.1 Coupled Air-Water Turbulent Couette Flow

We consider the Couette flows of air and water shown in Figure 1. The mean shear in the flow is maintained by the difference in the imposed (constant) velocities of the top boundary of the air and the bottom boundary of the water. There is no mean pressure gradient in the streamwise direction. From high-resolution simulation of this flow over long duration, we obtain detailed description of statistical, structural and dynamical characteristics of coupled air-water flows at low Froude numbers.

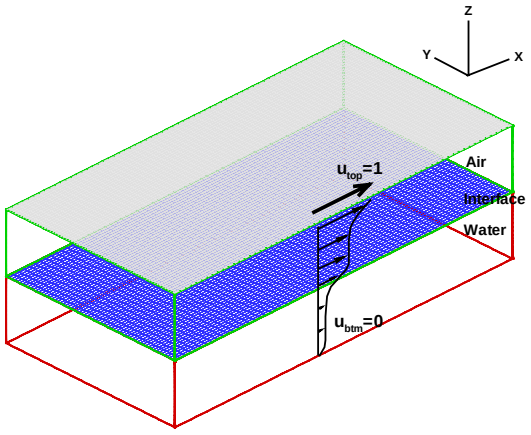

Figure 1: Schematics of coupled air-water turbulent Couette flow.

For the turbulence kinetic energy (TKE), $k = \overline{u_i' u_i'}/2$, its budget equation is given by:

$$\frac{dk}{dt} = P_k + \Pi_k + T_k + D_k + \varepsilon_k$$

where $P_k = -\overline{u_i' u_j'} \frac{\partial \overline{u}_i}{\partial x_j}$ is the turbulence energy production, $\Pi_k = -\frac{1}{\rho}\frac{\partial \overline{p' u_i'}}{\partial x_i}$ the transport due to pressure fluctuations, $T_k = -\frac{1}{2}\frac{\partial \overline{u_i' u_i' u_j'}}{\partial x_j}$ the transport due to velocity fluctuations, $D_k = \frac{1}{2}\nu \frac{\partial^2 \overline{u_i' u_i'}}{\partial x_j \partial x_j}$ the viscous diffusion, and $\varepsilon_k = -\nu \overline{\frac{\partial u_i'}{\partial x_j}\frac{\partial u_i'}{\partial x_j}}$ the turbulent energy dissipation.

Figure 2 shows profiles of each term in the TKE equation. Energy production is largest at locations close to the air-water interface, but reduces rapidly as the interface is approached. On the airside, dissipation increases towards the interface and reaches a maximum at the interface; turbulent velocity fluctuations transport TKE from the bulk region to the near-surface region. On the waterside, as the interface is approached, dissipation decreases first and then increases; a portion of the TKE from the near-surface region is transported to the bulk flow by turbulent velocity fluctuations. Viscous diffusion is only significant very close to the interface while in general, pressure transport is found to be much smaller than other processes.

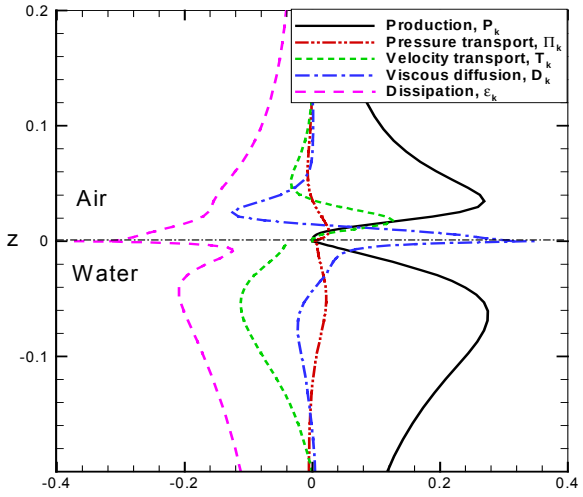

Figure 2: Variations of terms in the turbulent kinetic energy budget as functions of the distance from the interface. All the terms are normalized by u_τ^4/ν, with u_τ the shear velocity at the interface and ν the kinematic viscosity.

The three-dimensional, instantaneous flow field obtained from the simulation also provides detailed turbulence structures in the coupled air-water flow. Figure 3 shows an example of the instantaneous vortices in the vicinity of the interface. The vortical structures are represented by the isosurfaces of the second largest eigenvalue of $\underline{S}^2+\underline{\Omega}^2$, with $\underline{S}$ and $\underline{\Omega}$ the strain rate and the vorticity tensors, respectively (Jeong & Hussain 1995). On the airside, the vortices are mostly streamwise ones which are part of hairpin vortices, resembling what have been observed in boundary layers at a solid wall. On the waterside, the dominant vortices are hairpin vortices with the head portion located near the interface (shown in the center region of Figure 3) and surface-connected vortices (not shown in Figure 3). The two types of vortices are similar to the ones discovered in shear-free free-surface flows (Shen et al. 1999). The vortices in this flow, however, are stretched significantly in the streamwise direction due to the strong shear at the interface.

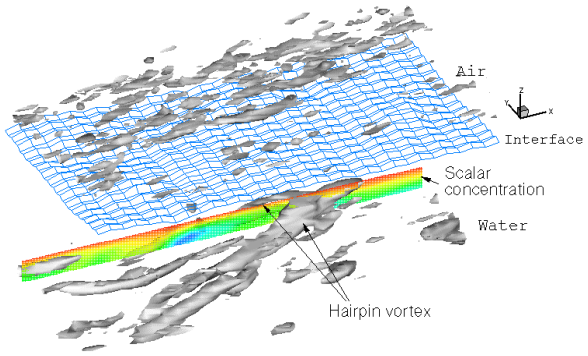

Figure 3: Vortex structures in the air and water near the interface, and scalar concentration on the vertical cross-section cutting through the head portion of a hairpin-shaped vortex.

The existence of these vortical structures can also be confirmed by the histogram statistics of vortex inclination angles. Using the approach of Moin & Kim (1985), we define the two-dimensional vortex inclination angles the same way as Shen et al. (1999) shown in Figure 4. Figure 5 shows that near the interface, θ_{yz} is concentrated around $90°$, signifying the presence of strong shear at the interface and the existence of hairpin heads. In the air close to the interface, θ_{xz} is centered around $90°$ and $270°$ corresponding to streamwise vortices. In the water, however, θ_{xz} has peaks around $0°/360°$ and $180°$. This

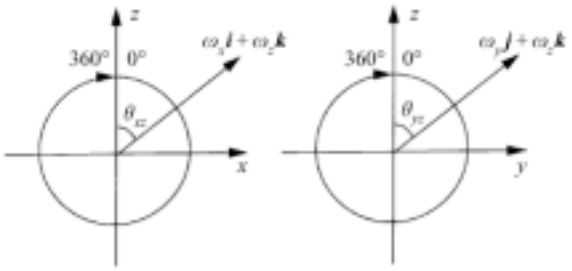

Figure 4: Definition of two-dimensional vortex inclination angles. Here θ_{xz} is the angle from the positive-z axis to the vorticity vector projected onto the (x,z)-plane, $\omega_x\hat{i}+\omega_z\hat{k}$, and θ_{yz} is the angle from the positive-z axis to the vorticity vector projected onto the (y,z)-plane, $\omega_y\hat{j}+\omega_z\hat{k}$.

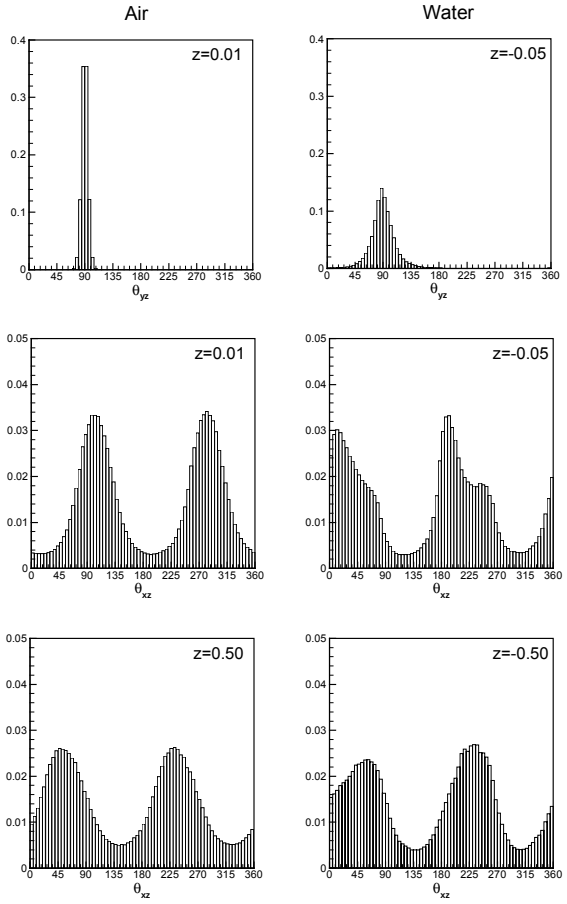

Figure 5: Histograms of vortex inclination angles, θ_{yz} in the (y,z)-plane and θ_{xz} in the (x,z)-plane, at various distances from the interface.

indicates the presence of surface-connected vortices ($|\omega_z| >> |\omega_x|$). Far away from the interface, θ_{xz} is centered around $45°$ and $225°$, showing the inclination of vortices with the bulk shear flow.

The vortical structures discussed above are found to play an essential role in the interfacial scalar transport. Figure 3 shows a typical example. On the vertical cross-section cutting through the hairpin vortex, the scalar concentration is plotted. It can be seen that upstream the hairpin vortex, the scalar boundary layer is thinned. This is caused by the upward convection of the scalar by the upwelling motions induced by the hairpin vortex. As a result, scalar transfer is enhanced there. For the same reason, the scalar boundary layer is thickened downstream the vortex and scalar transfer rate is reduced.

3.2 Steep Waves and Spilling Breaking Waves

In our numerical study, we generate a spilling breaking wave by starting an overly steep Airy wave. The evolution of the wave is then simulated with the EICM approach. The wave steepens and starts to break due to the interaction between the progressive wave and the (initially generated) standing wave as well as an excess amount of energy. There is no air entrainment in this particular case, although our experience shows that the EICM is also capable of capturing plunging breakers (Hendrickson 2004).

Figure 6 shows the detailed velocity and vorticity fields obtained from the simulation. The spilling breaking wave in this case is extremely strong and is marked by a flow separation in the water near the frontal face of the wave. As the wave evolves, the separation region moves down the wave face. It is found that this flow separation is a source of significant influx of vorticity for the water, because the surface parallel velocity is unable to follow the curvature up the front face of the wave. The face of the wave is a source of vorticity for the air in that it acts like a solid wall. Also shown in Figure 6 is the comparison between our numerical results and the experimental measurements performed by Qiao & Duncan (2001). It can be seen that the agreement is satisfactory.

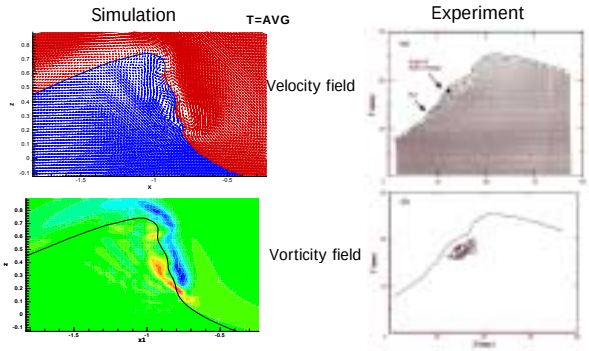

Figure 6: Velocity and vorticity fields in a steep breaking surface wave.

Based on the simulation results of the spilling breaker and the physical insights obtained, we further investigate the turbulence RANS modeling. RANS simulation of strong free-surface flows has been a formidable task despite its significant importance in applications. Recently, Brocchini & Peregrine (2001) developed a novel RANS formulation for such flows. They pointed out that our current understanding of this type of flows is far from sufficient. There is a critical need for the study of air-water-wave interaction dynamics, so that physics-based RANS modeling can be developed.

From the direct simulation of the spilling breaking waves, we perform phase-weighted Reynolds averaging of the flow field and are able to illustrate the characteristics of each term in the RANS equation. Figure 7 shows representative results. It is found that although globally the turbulence dissipation, production and transport are balanced, locally these terms are highly uncorrelated. This feature suggests that the non-local equilibrium nature of the spilling breaking wave must be captured in the turbulence modeling. Figure 7 also illustrates the interfacial pressure transport. This term is unique to air-water mixing flow. It was first identified by Brocchini & Peregrine (2001), while they were unable to evaluate its importance due to the lack of measurement data. Through this study, it is discovered that the interfacial pressure transport is much more significant than other interfacial transport processes, and it is even comparable in magnitude to traditional (for the bulk flow) turbulent transport term. Figure 7 shows that the interfacial pressure transport is negative (from water to air) due to a correlation between pressure fluctuations and surface-normal velocity fluctuations in the mixing zone.

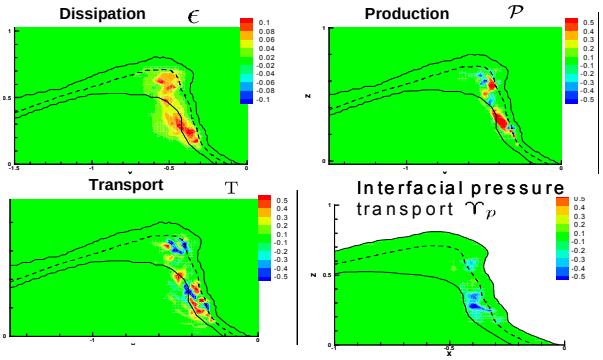

Figure 7: Turbulence dissipation, production, (traditional) transport, and interfacial pressure transport in a spilling breaking wave.

4. CONCLUSIONS

In this study we employ a systematic approach involving DNS, LES and RANS to investigate atmosphere-ocean-wave interactions at small scales. Simulations of a coupled air-water turbulent Couette flow show that the interface acts like a solid wall to the air motions. For the water motions, the interactions are intermediate between but qualitatively distinct from those at a shear-free free surface and a solid wall. Characteristics of the structures, statistics and dynamics of air-water interactions at low Froude numbers have been identified. For moderate to high Froude numbers, we develop a novel Eulerian interface capturing method to study air-water-wave interactions. Our simulation of an unsteady spilling breaking wave elucidates detailed flow structures, based on which turbulent kinetic energy balance is analyzed. The results obtained in this study are useful for the development of efficacious turbulence modeling of air-sea wave boundary layer.

ACKNOWLEDGEMENTS

This research is financially supported by the CBLAST project of the Office of Naval Research with a portion of the computational resources provided by ONR through the DoD HPCMP program.

REFERENCES

Brocchini, M. & Peregrine, D. H., 2001: The dynamics of strong turbulence at free surfaces. Part 2. Free-surface boundary conditions. *J. Fluid Mech*., **449**, 255−290.

Jeong, J. & Hussain, F., 1995: On the identification of a vortex. *J. Fluid Mech*., **285**, 69−94

Hendrickson, K., 2004: Numerical simulations of steep breaking waves. *Ph.D. Thesis*, Dept. of Ocean. Eng., MIT.

Moin, P. & Kim, J., 1985: The structure of the vorticity field in turbulent channel flow. Part 1. Analysis of instantaneous fields and statistical correlations. *J. Fluid Mech*., **155**, 441−464.

Qiao, H. & Duncan, J. H., 2001: Gentle spilling breakers: crest flow-field evolution. *J. Fluid Mech*., **439**, 57-85.

Shen, L. & Yue, D. K. P., 2001: Large-eddy simulation of free-surface turbulence. *J. Fluid Mech*., **440**, 75−116.

Shen, L., Zhang, X., Yue, D. K. P. & Triantafyllou, G. S., 1999: The surface layer for free-surface turbulent flows. *J. Fluid Mech*., **386**, 167−212.